

# Peristaltic Transport of a Nanofluid in an Inclined Tube

K. Maruthi Prasad<sup>1,\*</sup>, N. Subadra<sup>2</sup>, M. A. S. Srinivas<sup>3</sup>

<sup>1</sup>Department of Engineering Mathematics, GITAM University, Hyderabad Campus, Hyderabad, Telangana, India

<sup>2</sup>Department of Mathematics, Geethanjali College of Engg. & Tech., Cheeryal (V), Keesara (M), R.R. Dist., Telangana, India

<sup>3</sup>Department of Mathematics, Jawaharlal Nehru Technological University, Kukatpally, Hyderabad, Telangana, India

**Abstract** Peristaltic transport of a nanofluid in an inclined tube under the assumption of long wave length and low Reynolds number has been investigated. The coupled equations in temperature profile and nanoparticle phenomena are solved by using Homotopy Perturbation Method. By using this method the closed form solutions of pressure drop, time averaged flux and frictional force have been calculated. It is found that the pressure drop increases with the Brownian motion parameter  $N_b$  but decreases with the thermophoresis number  $N_t$  and inclination  $\alpha$ . It is also found that the pressure drop decreases with wave amplitude and increases with wave length. The frictional force increases with Brownian motion parameter  $N_b$ , wavelength and decreases with the thermophoresis number  $N_t$ , inclination  $\alpha$  and wave amplitude. It can be seen that, the temperature profile decreases with the Brownian motion parameter  $N_b$  and increases with the thermophoresis number  $N_t$ . The nanoparticle phenomena increases with the Brownian motion parameter  $N_b$  and decreases with the thermophoresis number  $N_t$ . It is observed that, the maximum pressure gradient occurs for different values of wave amplitude for sinusoidal, multi sinusoidal, triangular, trapezoidal and square waves. The size of the trapped bolus in multi sinusoidal wave is small as compared to the sinusoidal wave.

**Keywords** Peristalsis, Nanofluid, Homotopy perturbation method, Brownian motion parameter, Thermophoresis number

## 1. Introduction

The study of peristaltic transport has received considerable attention in the recent past, as it is known to be one of the main mechanisms for fluid transport in biological systems. It is found that physiological flows are maintained by sinusoidal pressure gradient as well as motion of the boundaries. Peristaltic transport widely occurs in many biological systems as well as in many industries. For example, food swallowing through the esophagus, intra-urine fluid motion, circulation of blood in small blood vessels, the flow of many other glandular ducts and toxic liquid transportation in the nuclear industry etc.

Peristalsis was first studied by Latham [11] in 1965. He analyzed the fluid motion in a peristaltic pump. Several investigators have contributed to the study of peristaltic motion in both mechanical and physiological situations. Shapiro et al. [20], Fung and Yih [5], Radhakrishnamacharya and Srinivasulu [19], Misra et al. [16], Mekheimer [15].

Though all the above investigations consider the fluid to be Newtonian, some researchers studied peristaltic transport of non-Newtonian fluids also: Devi and Devanathan [4], Srivastava and Srivastava [21], Muthu et al. [17], Maruthi

Prasad and Radhakrishnamacharya [12]. Maruthi Prasad et al. [14] studied unsteady peristaltic flow of a viscous fluid in a two dimensional curved channel.

In recent days many researchers have focused their attention on the study of nanofluid for different flow geometries. Choi [2] was first person who initiated to study the nanofluid technology. A detailed examination of nanofluid was discussed by Buongiorno J [1] in Convective transport in nanofluids. Das et al. [3] studied Pool boiling of nanofluids on horizontal narrow tubes. Noreen Sher Akbar et al. [18] studied Peristaltic flow of a nanofluid in a non-uniform tube. They analyzed the temperature profile and nanoparticle phenomena using homotopy perturbation technique. Khan and Pop [9] studied boundary layer flow of a nanofluid passing a stretching sheet.

It is known that many ducts in physiological systems are not horizontal but have some inclination with the axis. Maruthi Prasad K et al. [13] studied Peristaltic pumping of a micropolar fluid in an inclined tube. However, the study of peristaltic transport of a nanofluid in an inclined tube has not been studied.

Motivated by these studies, the peristaltic pumping of a nanofluid in an inclined tube under the assumption of long wavelength and low Reynolds number is investigated. The resulting equations of the temperature profile and nanoparticle phenomena are solved using homotopy perturbation technique. The analytical solutions of velocity, pressure drop and frictional forces are obtained. The effects

\* Corresponding author:

kaipa\_maruthi@yahoo.com (K. Maruthi Prasad)

Published online at <http://journal.sapub.org/ajcam>

Copyright © 2015 Scientific & Academic Publishing. All Rights Reserved

of various parameters on these flow variables are investigated. The pressure gradient versus sinusoidal wave, multi sinusoidal wave, triangular wave, trapezoidal wave and square wave are presented graphically. The stream lines for sinusoidal wave and multi sinusoidal waves are represented graphically at the end.

## 2. Physical Model and Fundamental Equations

Equations for an incompressible fluid for the balance of mass, momentum, temperature and nanoparticle volume fraction are given by [10]

$$\begin{aligned} \text{div} \bar{V} &= 0, \\ \rho_f \frac{d\bar{V}}{dt} &= -\nabla \bar{p} + \mu \nabla^2 \bar{V} + f, \\ (\rho c)_f \frac{d\bar{T}}{dt} &= k \nabla^2 \bar{T} + (\rho c)_p [D_B \nabla \bar{C} \cdot \nabla \bar{T} + \frac{D_T}{T_o} \nabla \bar{T} \cdot \nabla \bar{T}], \\ \frac{d\bar{C}}{dt} &= D_B \nabla^2 \bar{C} + \left[ \frac{D_T}{T_o} \right] \nabla^2 \bar{T}, \end{aligned}$$

where  $\rho_f$  is the density of the fluid,  $\rho_p$  is the density of the particle,  $C$  is the volumetric volume expansion coefficient,  $\bar{V}$  is the velocity vector,  $f$  is the body forces,  $\frac{d}{dt}$  represents the material time derivative,  $\bar{p}$  is the pressure,  $\bar{C}$  is the nanoparticle phenomena,  $D_B$  is the Brownian diffusion coefficient and  $D_T$  is the thermophoretic diffusion coefficient. The ambient values of  $\bar{T}$  and  $\bar{C}$  as  $\bar{r}$  tend to  $\bar{h}$  are denoted by  $\bar{T}_o$  and  $\bar{C}_o$ .

## 3. Mathematical Formulation

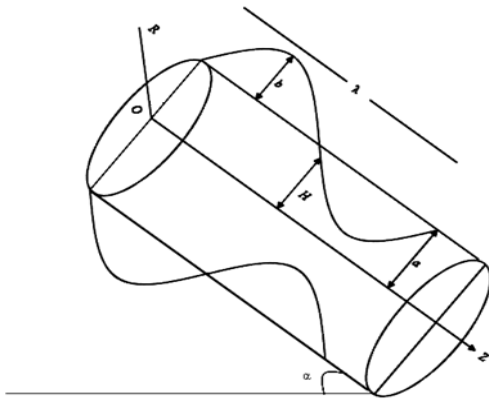


Figure 1. Peristaltic transport in an inclined tube

Consider the peristaltic motion of an incompressible nanofluid in an inclined tube of uniform cross-section of radius ' $a$ ' with sinusoidal waves travelling along the tube with speed  $c_1$ , amplitude  $b$  and wave length  $\lambda$ . Further suppose the tube is inclined at an angle  $\alpha$  with the horizontal axis as shown in Figure 1. Heat transfer and nano-particle phenomena are considered. At the center of the

tube, symmetry condition is used on both temperature and concentration, while the walls of the tube maintain temperature  $\bar{T}_o$  and nanoparticle volume fraction  $\bar{C}_o$ .

The geometry of the wall surface is defined as

$$H(z, t) = a(\bar{Z}) + b \sin \frac{2\pi}{\lambda} (\bar{Z} - c_1 \bar{t}), \quad (1)$$

where  $a(\bar{Z}) = a + k\bar{Z}$ , ' $a$ ' is the radius of the inlet,  $k$  is the constant whose magnitude depends on the length of the tube and  $\bar{t}$  is the time. Cylindrical coordinate system  $(\bar{R}, \bar{Z})$  is chosen, so that  $Z$ -axis coincides with the center line of the tube and  $\bar{R}$  is transverse to it. Further, the flow is assumed to be axisymmetric.

Using the transformations

$$\bar{z} = \bar{Z} - c_1 \bar{t}, \quad \bar{r} = \bar{R}, \quad (2)$$

$$\bar{w} = \bar{W} - c_1, \quad \bar{u} = \bar{U}. \quad (3)$$

From a stationary to a moving frame of reference, where  $\bar{U}, \bar{W}$  and  $\bar{u}, \bar{w}$  are velocity components in the radial and axial directions in the fixed and moving frames respectively, the governing equations in a fixed frame for an incompressible nanofluid in an inclined tube are given by

$$\frac{1}{\bar{r}} \frac{\partial(\bar{r}\bar{u})}{\partial \bar{r}} + \frac{\partial \bar{w}}{\partial \bar{z}} = 0, \quad (4)$$

$$\begin{aligned} \rho \left[ \bar{u} \frac{\partial \bar{u}}{\partial \bar{r}} + \bar{w} \frac{\partial \bar{u}}{\partial \bar{z}} \right] &= -\frac{\partial \bar{P}}{\partial \bar{r}} + \mu \left[ \frac{\partial^2 \bar{u}}{\partial \bar{r}^2} + \frac{1}{\bar{r}} \frac{\partial \bar{u}}{\partial \bar{r}} + \frac{\partial^2 \bar{u}}{\partial \bar{z}^2} - \frac{\bar{u}}{\bar{r}^2} \right] - \frac{\cos \alpha}{F}, \end{aligned} \quad (5)$$

$$\begin{aligned} \rho \left[ \bar{u} \frac{\partial \bar{w}}{\partial \bar{r}} + \bar{w} \frac{\partial \bar{w}}{\partial \bar{z}} \right] &= -\frac{\partial \bar{P}}{\partial \bar{z}} + \mu \left[ \frac{\partial^2 \bar{w}}{\partial \bar{r}^2} + \frac{1}{\bar{r}} \frac{\partial \bar{w}}{\partial \bar{r}} + \frac{\partial^2 \bar{w}}{\partial \bar{z}^2} \right] \\ &+ \rho g \alpha (\bar{T} - \bar{T}_o) + \rho g \alpha (\bar{C} - \bar{C}_o) + \frac{\sin \alpha}{F}, \end{aligned} \quad (6)$$

$$\begin{aligned} \left[ \bar{u} \frac{\partial \bar{T}}{\partial \bar{r}} + \bar{w} \frac{\partial \bar{T}}{\partial \bar{z}} \right] &= \alpha \left[ \frac{\partial^2 \bar{T}}{\partial \bar{r}^2} + \frac{1}{\bar{r}} \frac{\partial \bar{T}}{\partial \bar{r}} + \frac{\partial^2 \bar{T}}{\partial \bar{z}^2} \right] \\ &+ \tau \left\{ D_B \left[ \frac{\partial \bar{C}}{\partial \bar{r}} \frac{\partial \bar{T}}{\partial \bar{r}} + \frac{\partial \bar{C}}{\partial \bar{z}} \frac{\partial \bar{T}}{\partial \bar{z}} \right] + \frac{D_T}{T_o} \left[ \left( \frac{\partial \bar{T}}{\partial \bar{r}} \right)^2 + \left( \frac{\partial \bar{T}}{\partial \bar{z}} \right)^2 \right] \right\}, \end{aligned} \quad (7)$$

$$\begin{aligned} \left[ \bar{u} \frac{\partial \bar{C}}{\partial \bar{r}} + \bar{w} \frac{\partial \bar{C}}{\partial \bar{z}} \right] &= D_B \left[ \frac{\partial^2 \bar{C}}{\partial \bar{r}^2} + \frac{1}{\bar{r}} \frac{\partial \bar{C}}{\partial \bar{r}} + \frac{\partial^2 \bar{C}}{\partial \bar{z}^2} \right] \\ &+ \frac{D_T}{T_o} \left[ \frac{\partial^2 \bar{T}}{\partial \bar{r}^2} + \frac{1}{\bar{r}} \frac{\partial \bar{T}}{\partial \bar{r}} + \frac{\partial^2 \bar{T}}{\partial \bar{z}^2} \right], \end{aligned} \quad (8)$$

where  $\tau = \frac{(\rho c)_p}{(\rho c)_f}$  is the ratio between the effective heat capacity of the nanoparticle material and heat capacity of the fluid.

The boundary conditions in the wave frame are as follows

$$\frac{\partial \bar{w}}{\partial \bar{r}} = 0, \quad \frac{\partial \bar{T}}{\partial \bar{r}} = 0, \quad \frac{\partial \bar{C}}{\partial \bar{r}} = 0 \text{ at } \bar{r} = 0. \quad (9)$$

$$\bar{w} = 0, \quad \bar{T} = \bar{T}_o, \quad \bar{C} = \bar{C}_o \text{ at } \bar{r} = \bar{h} = a(\bar{z}) + b \sin \frac{2\pi}{\lambda} (\bar{z}). \quad (10)$$

The following are non-dimensional variables:

$$\begin{aligned} R &= \frac{\bar{R}}{a}, \quad r = \frac{\bar{r}}{a}, \quad Z = \frac{\bar{Z}}{\lambda}, \quad z = \frac{\bar{z}}{\lambda}, \\ W &= \frac{\bar{W}}{c_1}, \quad w = \frac{\bar{w}}{c_1}, \quad U = \frac{\lambda \bar{U}}{a c_1}, \quad u = \frac{\lambda \bar{u}}{a c_1} \end{aligned}$$

$$\begin{aligned}
p &= \frac{a^2 \bar{p}}{c_1 \lambda \mu}, \theta = \frac{\bar{T} - \bar{T}_o}{\bar{T}_o}, t = \frac{c_1 \bar{t}}{\lambda}, \\
\delta &= \frac{a}{\lambda}, R_e = \frac{2\rho c_1 a}{\mu}, \sigma = \frac{\bar{C} - \bar{C}_o}{\bar{C}_o}, \\
h &= \frac{\bar{h}}{a} = 1 + \frac{\lambda k z}{a_o} + \phi \sin 2\pi z, \beta = \frac{k}{(\rho C)_f}, \\
N_b &= \frac{(\rho C)_p D_B \bar{C}_o}{(\rho C)_f}, N_t = \frac{(\rho C)_p D_T \bar{T}_o}{(\rho C)_f \beta}, \\
P_r &= \frac{\gamma}{\beta}, G_r = \frac{g \beta a^3 \bar{T}_o}{\gamma^2}, B_r = \frac{g \beta a^3 \bar{C}_o}{\gamma^2}, \quad (11)
\end{aligned}$$

in which  $P_r, N_b, N_t, G_r$  and  $B_r$  are the Prandtl number, the Brownian motion parameter, the thermophoresis parameter, local temperature Grashof number and local nanoparticle Grashof number.

Introducing the non-dimensional variables into equations (4)-(10) under the assumption of long wave length and low Reynolds number approximations, the equations (4)-(10) reduces to

$$\frac{\partial u}{\partial r} + \frac{u}{r} + \frac{\partial w}{\partial z} = 0, \quad (12)$$

$$\frac{\partial P}{\partial r} = -\frac{\cos \alpha}{F}, \quad (13)$$

$$\frac{\partial P}{\partial z} - \frac{\sin \alpha}{F} = \frac{1}{r} \frac{\partial}{\partial r} \left( r \frac{\partial w}{\partial r} \right) + G_r \theta + B_r \sigma, \quad (14)$$

$$0 = \frac{1}{r} \frac{\partial}{\partial r} \left( r \frac{\partial \theta}{\partial r} \right) + N_b \frac{\partial \sigma}{\partial r} \frac{\partial \theta}{\partial r} + N_t \left( \frac{\partial \theta}{\partial r} \right)^2, \quad (15)$$

$$0 = \frac{1}{r} \frac{\partial}{\partial r} \left( r \frac{\partial \sigma}{\partial r} \right) + \frac{N_t}{N_b} \left( \frac{1}{r} \frac{\partial}{\partial r} \left( r \frac{\partial \theta}{\partial r} \right) \right), \quad (16)$$

From equation (13) it is clear that  $\frac{\partial P}{\partial z}$  is a function of  $z$  only.

The non-dimensional boundary conditions are

$$\frac{\partial w}{\partial r} = 0, \frac{\partial \theta}{\partial r} = 0, \frac{\partial \sigma}{\partial r} = 0 \text{ at } r = 0, \quad (17a)$$

$$w = 0, \theta = 0, \sigma = 0 \text{ at } r = h = 1 + \frac{\lambda k z}{a_o} + \phi \sin 2\pi z. \quad (17b)$$

## 4. Solution

The combination of the homotopy method and perturbation method is called Homotopy Perturbation Method (HPM). This method eliminates the drawbacks present in the traditional perturbation method and at the same time all the advantages remain the same.

The homotopy for the equations (15) and (16) are as follows [6-8]:

$$\begin{aligned}
H(q, \theta) &= (1 - q)[L(\theta) - L(\theta_{10})] \\
&+ q \left[ L(\theta) + N_b \frac{\partial \sigma}{\partial r} \frac{\partial \theta}{\partial r} + N_t \left( \frac{\partial \theta}{\partial r} \right)^2 \right]. \quad (18)
\end{aligned}$$

$$\begin{aligned}
H(q, \sigma) &= (1 - q)[L(\sigma) - L(\sigma_{10})] \\
&+ q \left[ L(\sigma) + \frac{N_t}{N_b} \left( \frac{1}{r} \frac{\partial}{\partial r} \left( r \frac{\partial \theta}{\partial r} \right) \right) \right]. \quad (19)
\end{aligned}$$

For convenience,  $L = \frac{1}{r} \frac{\partial}{\partial r} \left( r \frac{\partial}{\partial r} \right)$  is taken as linear operator.

$$\theta_{10}(r, z) = \left( \frac{r^2 - h^2}{4} \right), \quad \sigma_{10}(r, z) = - \left( \frac{r^2 - h^2}{4} \right) \quad (20)$$

are defined as initial guesses which satisfy the boundary conditions.

Define

$$\theta(r, z) = \theta_0 + q\theta_1 + q^2\theta_2 + \dots, \quad (21)$$

$$\sigma(r, z) = \sigma_0 + q\sigma_1 + q^2\sigma_2 + \dots. \quad (22)$$

The series (21) and (22) are convergent for most of the cases. The convergent rate depends on the nonlinear part of the equation.

Adopting the same procedure as done by HeJH [6-8], the solution for temperature and nanoparticle phenomena can be written for  $q=1$  as

$$\theta(r, z) = \left( \frac{r^4 - h^4}{64} \right) (N_b - N_t), \quad (23)$$

$$\sigma(r, z) = - \left( \frac{r^2 - h^2}{4} \right) \frac{N_t}{N_b}. \quad (24)$$

Substituting the equations (23) and (24) in the equation (14) and applying boundary conditions, the closed form of analytical solution for velocity can be written as

$$\begin{aligned}
w(r, z) &= \left( \frac{r^2 - h^2}{4} \right) \left( -\frac{\sin \alpha}{F} + \frac{dP}{dz} \right) \\
&+ B_r \frac{N_t}{N_b} \left( \frac{r^4}{64} - \frac{r^2 h^2}{16} + \frac{3h^4}{64} \right) \\
&- G_r (N_b - N_t) \left( \frac{r^6}{2304} - \frac{r^2 h^4}{256} + \frac{h^6}{288} \right). \quad (25)
\end{aligned}$$

The dimension less flux  $q$  in the moving frame is given by

$$q = \int_0^h 2r w dr. \quad (26)$$

By substituting equation (25) in equation (26), the flux value will be

$$\begin{aligned}
q &= -(0.125) \left( -\frac{\sin \alpha}{F} + \frac{dP}{dz} \right) h^4 \\
&+ B_r \frac{N_t}{N_b} h^6 (0.02083) + G_r (N_b - N_t) h^8 (0.01628). \quad (27)
\end{aligned}$$

From equation (27),  $\frac{dP}{dz}$  can be written as

$$\begin{aligned}
\frac{dP}{dz} &= -\frac{8q}{h^4} + \frac{\sin \alpha}{F} + (0.16664) B_r \frac{N_t}{N_b} h^2 \\
&+ (0.13024) G_r (N_b - N_t) h^4. \quad (28)
\end{aligned}$$

The pressure drop over a wave length  $\Delta P_\lambda$  is defined by

$$\Delta P_\lambda = - \int_0^1 \frac{dP}{dz} dz. \quad (29)$$

Substituting equation (28) in equation (29),  $\Delta P_\lambda$  can be written as

$$\Delta P_\lambda = q L_1 + L_2. \quad (30)$$

Where

$$L_1 = 8 \int_0^1 \frac{1}{h^4} dz \text{ and} \quad (31)$$

$$L_2 = \int_0^1 \left\{ -\frac{\sin \alpha}{F} - (0.16664)B_r \frac{N_t}{N_b} h^2 - (0.13024)G_r (N_b - N_t) h^4 dz \right\} \quad (32)$$

Following the analysis of Shapiro et al [20], the time averaged flux over a period in the laboratory frame  $\bar{Q}$  is given by

$$\bar{Q} = 1 + \frac{\epsilon^2}{2} + q \quad (33)$$

Substituting the value of  $q$  from equation (30) to equation (33), the equation of time averaged flux can be written as

$$\bar{Q} = 1 + \frac{\epsilon^2}{2} + \frac{\Delta P_\lambda}{L_1} - \frac{L_2}{L_1} \quad (34)$$

The dimensionless friction force  $\bar{F}$  at the wall is given by

$$\bar{F} = \int_0^1 h^2 \left( -\frac{dP}{dz} \right) dz. \quad (35)$$

Five wave forms have been considered for analysis of pressure gradient namely sinusoidal wave, multi sinusoidal wave, triangular wave, trapezoidal wave and square waves. The non-dimensional expressions for these wave forms are as follows:

1. Sinusoidal Wave:

$$h(z) = 1 + \frac{\lambda kz}{a_0} + \phi \sin(2\pi z)$$

2. Multi Sinusoidal Wave:

$$h(z) = 1 + \frac{\lambda kz}{a_0} + \phi \sin(2m\pi z)$$

3. Triangular Wave:

$$h(z) = 1 + \frac{\lambda kz}{a_0} + \phi \left\{ \frac{8}{\pi^3} \sum_{m=1}^{\infty} \frac{(-1)^{n+1}}{(2m-1)^2} \sin(2\pi(2m-1)z) \right\}$$

4. Trapezoidal Wave:

$$h(z) = 1 + \frac{\lambda kz}{a_0} + \phi \left\{ \frac{32}{\pi^2} \sum_{m=1}^{\infty} \frac{\sin \frac{\pi}{8} (2m-1)}{(2m-1)^2} \sin(2\pi(2m-1)z) \right\}$$

5. Square Wave:

$$h(z) = 1 + \frac{\lambda kz}{a_0} + \phi \left\{ \frac{4}{\pi} \sum_{m=1}^{\infty} \frac{(-1)^{n+1}}{2m-1} \cos(2\pi(2m-1)z) \right\}$$

## 5. Results and Discussions

Analytical solutions for pressure drop ( $\Delta P_\lambda$ ), time averaged flux ( $\bar{Q}$ ) and frictional forces ( $\bar{F}$ ) are given by the equations (23), (34) and (35) respectively. The effects of various parameters on pressure drop ( $\Delta P_\lambda$ ), time averaged flux ( $\bar{Q}$ ), frictional force ( $\bar{F}$ ), temperature profile and nanoparticle phenomena have been calculated numerically

by using Mathematica 9.0 software and the results are graphically presented in figures 2(a)-5(b). The pressure gradient for sinusoidal wave, multi sinusoidal wave, triangular wave, trapezoidal wave and square waves has been graphically represented from figures 6(a)-6(e). Stream lines for sinusoidal and multi sinusoidal waves are represented from figures 7(a)-7(b).

The effects of various parameters on the pressure drop ( $\Delta P_\lambda$ ) are shown in figures 2(a)-2(e), for various values of Brownian motion number ( $N_b$ ), thermophoresis parameter ( $N_t$ ), inclination ( $\alpha$ ), wave length ( $\lambda$ ) and wave amplitude ( $\phi$ ). It is observed that pressure drop increases with Brownian motion number ( $N_b$ ) but decreases with thermophoresis parameter ( $N_t$ ) and inclination ( $\alpha$ ). Pressure drop ( $\Delta P_\lambda$ ) decreases with wave amplitude ( $\phi$ ) and increases with wave length ( $\lambda$ ) but it is interesting to note that the pressure drop converges to a particular value when the value of  $\bar{Q}$  exceeds 1.

Figures 3(a)-3(e) represent the behaviour of frictional force ( $\bar{F}$ ) for different values of Brownian motion number ( $N_b$ ), thermophoresis parameter ( $N_t$ ), inclination ( $\alpha$ ), wave length ( $\lambda$ ) and wave amplitude ( $\phi$ ). It is observed that frictional force increases with the Brownian motion number ( $N_b$ ) but decreases with the thermophoresis parameter ( $N_t$ ) and inclination ( $\alpha$ ). Frictional force ( $\bar{F}$ ) decreases with wave amplitude ( $\phi$ ) and increases with wave length ( $\lambda$ ) but converges to a particular value when  $\bar{Q}$  exceeds 1.

It can be seen from figures 4(a)-4(b) that, temperature profile ( $\theta$ ) decreases with the Brownian motion parameter ( $N_b$ ) whereas increases with the thermophoresis parameter ( $N_t$ ).

Nanoparticle phenomena ( $\sigma$ ) has been shown from figures 5(a)-5(b) for different values of Brownian motion number ( $N_b$ ) and thermophoresis parameter ( $N_t$ ). It is observed that nanoparticle phenomena increases with the Brownian motion parameter ( $N_b$ ) but decreases with the thermophoresis parameter ( $N_t$ ). From the graphs it is interested to note that the temperature profile has an opposite behaviour as compared to the nanoparticle phenomena.

Pressure gradient ( $\frac{dP}{dz}$ ) has been presented from figures 6(a)-6(e) for different values of wave amplitude ( $\phi$ ) for sinusoidal wave, multi sinusoidal wave, triangular wave, trapezoidal wave and square waves. Maximum pressure gradient occurs in sinusoidal wave, triangular wave and trapezoidal waves for  $z \in [0.5, 1]$  but interestingly for square wave pressure gradient ( $\frac{dP}{dz}$ ) is maximum for  $z \in [0.25, 0.75]$  whereas for multi sinusoidal wave, the pressure gradient ( $\frac{dP}{dz}$ ) is maximum for  $z \in [0.25, 0.5]$ .

Figures 7(a)-7(b) shows streamlines for sinusoidal and multi sinusoidal waves. It is noticed that the size of the trapped bolus in multi sinusoidal wave is small as compared to the sinusoidal wave.

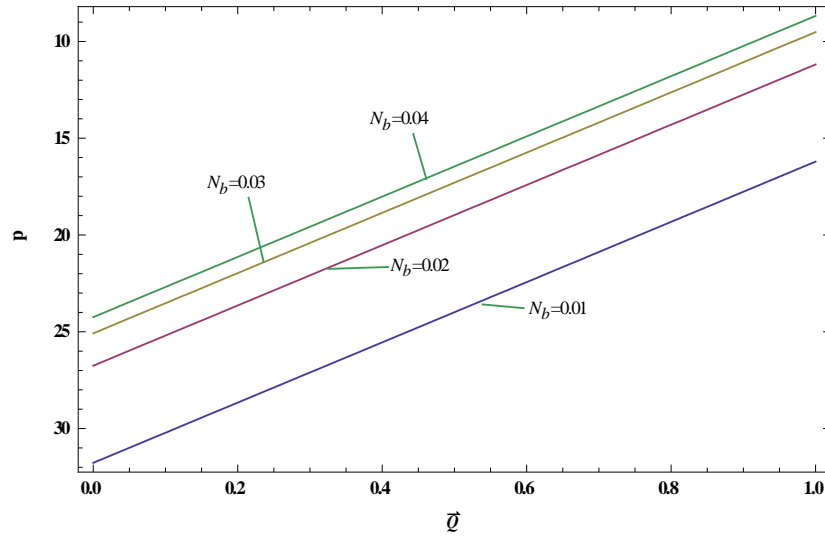


**Figure 2(a).** Effect of  $\bar{Q}$  and  $(\Delta P_\lambda)$  ( $N_t = 1.8, G_r = 0.2, B_r = 0.3, \alpha = 30^\circ, \epsilon = 0.4, F = 0.1, k = 0.04, \lambda = 0.01, \phi = 0.4, a_0 = 0.01$ )

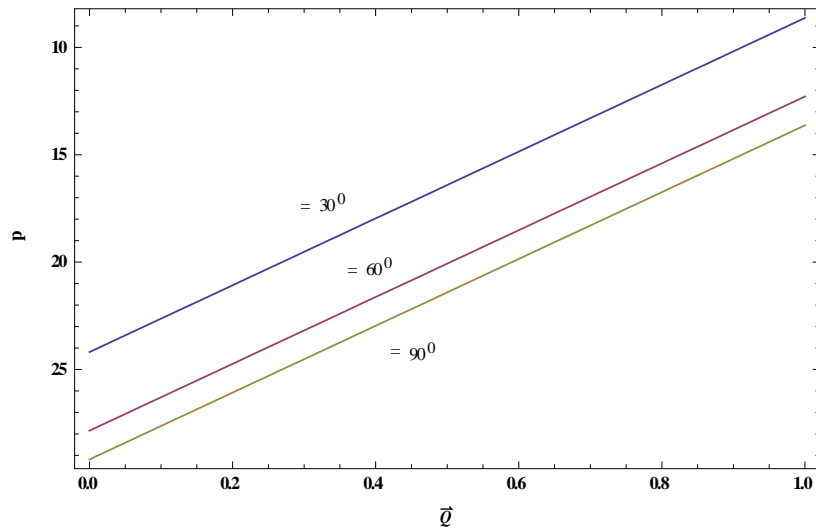


**Figure 2(b).** Effect of  $\bar{Q}$  and  $(\Delta P_\lambda)$  ( $N_b = 0.1, G_r = 0.2, B_r = 0.3, \alpha = 30^\circ, \epsilon = 0.4, F = 0.1, k = 0.04, \lambda = 0.01, \phi = 0.4, a_0 = 0.01$ )

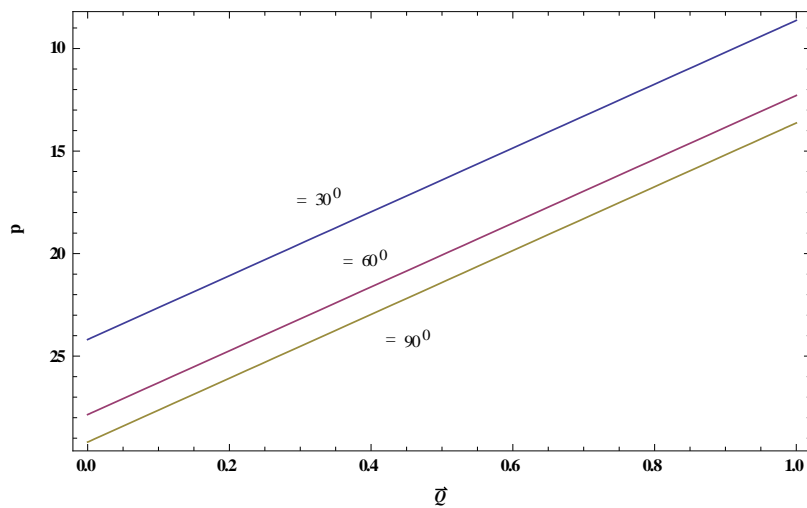


**Figure 2(c).** Effect of  $\bar{Q}$  and  $\Delta P_\lambda$  ( $N_b = 0.1, N_t = 4.6, G_r = 0.2, B_r = 0.3, \epsilon = 0.4, F = 0.1, k = 0.04, \lambda = 0.01, \phi = 0.4, a_0 = 0.01$ )

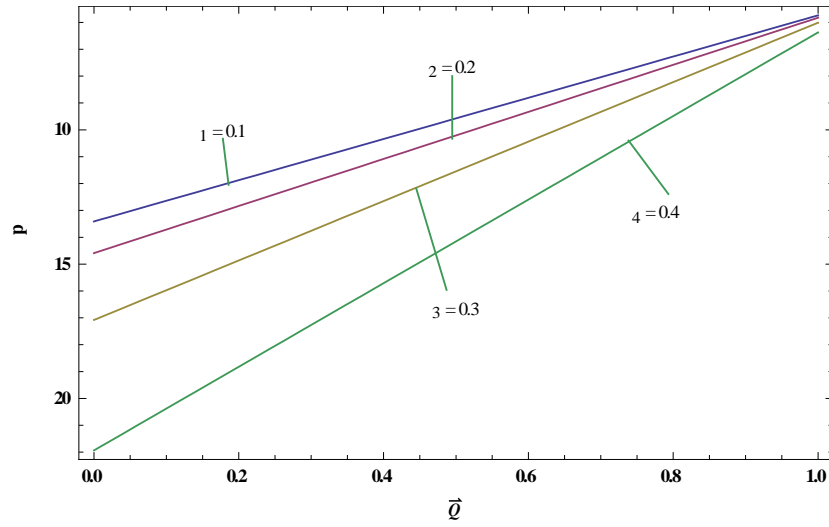


**Figure 2(d).** Effect of  $\bar{Q}$  and  $\Delta P_\lambda$  ( $N_b = 0.3, N_t = 0.8, G_r = 0.2, B_r = 0.3, \alpha = 30^\circ, \epsilon = 0.4, F = 0.1, k = 0.04, \lambda = 0.01, a_0 = 0.01$ )

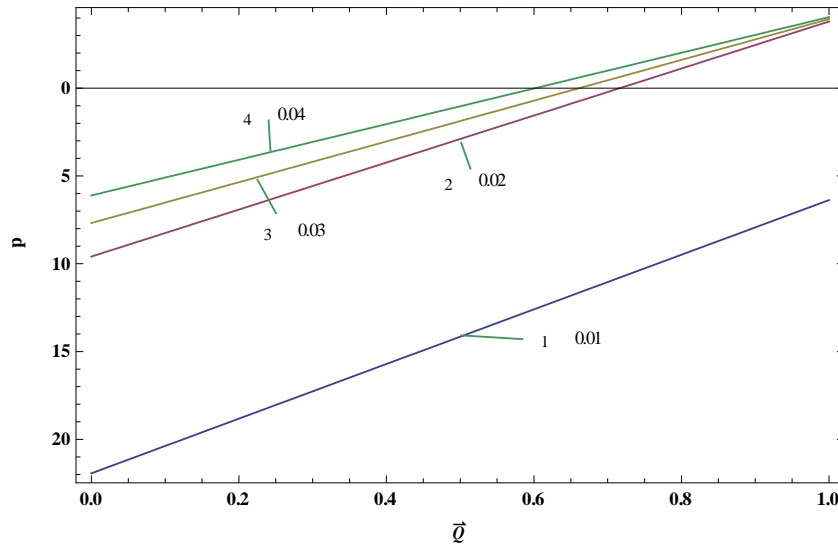


**Figure 2(e).** Effect of  $\bar{Q}$  and  $\Delta P_\lambda$  ( $N_b = 0.3, N_t = 0.8, G_r = 0.2, B_r = 0.3, \alpha = 30^\circ, \epsilon = 0.4, F = 0.1, k = 0.04, a_0 = 0.01, \phi = 0.4$ )

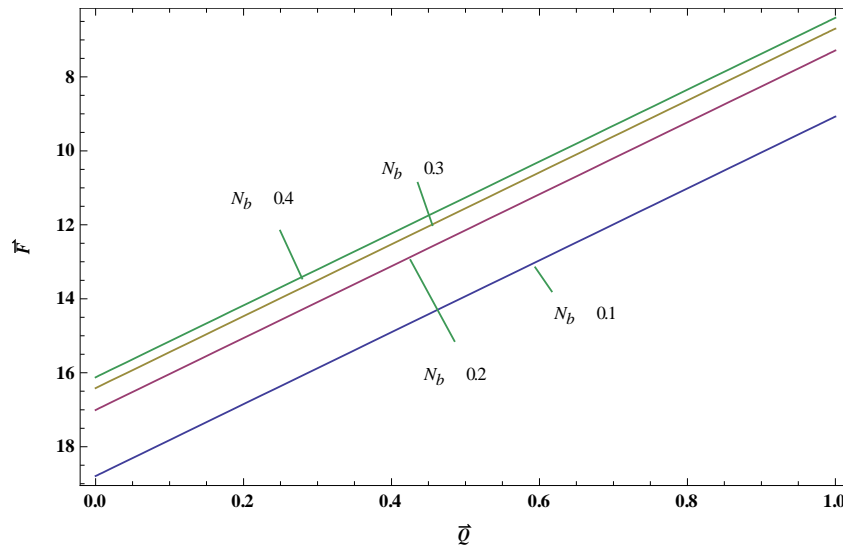


**Figure 3(a).** Effect of  $\bar{Q}$  and  $\bar{F}$  ( $N_t = 4.6, G_r = 0.2, B_r = 0.3, \alpha = 30^\circ, \epsilon = 0.4, F = 0.1, k = 0.04, \lambda = 0.01, \phi = 0.4, a_0 = 0.01$ )

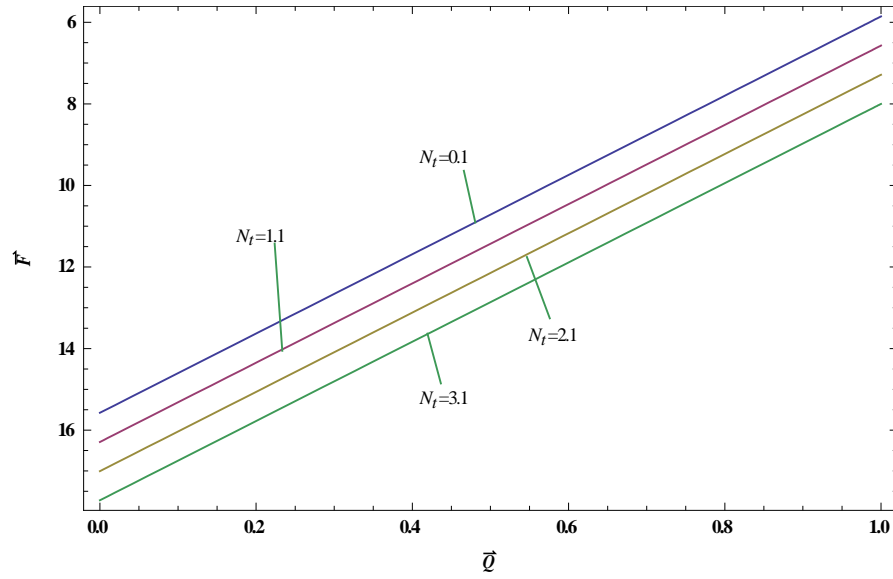


**Figure 3(b).** Effect of  $\bar{Q}$  and  $\bar{F}$  ( $N_b = 0.1, G_r = 0.2, B_r = 0.3, \alpha = 30^\circ, \epsilon = 0.4, F = 0.1, k = 0.04, \lambda = 0.01, \phi = 0.4, a_0 = 0.01$ )

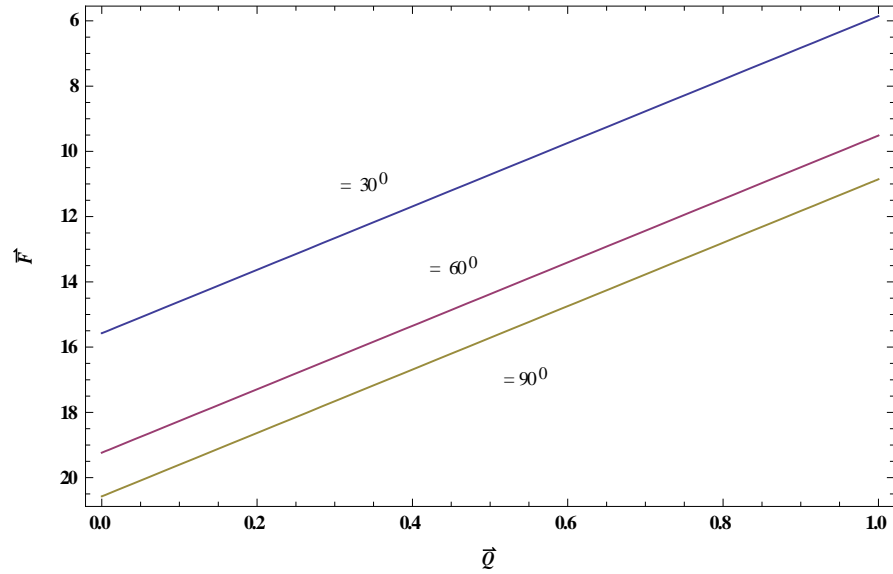


**Figure 3(c).** Effect of  $\bar{Q}$  and  $\bar{F}$  ( $N_b = 0.1, N_t = 0.1, G_r = 0.2, B_r = 0.3, \epsilon = 0.4, F = 0.1, k = 0.04, \lambda = 0.01, \phi = 0.4, a_0 = 0.01$ )

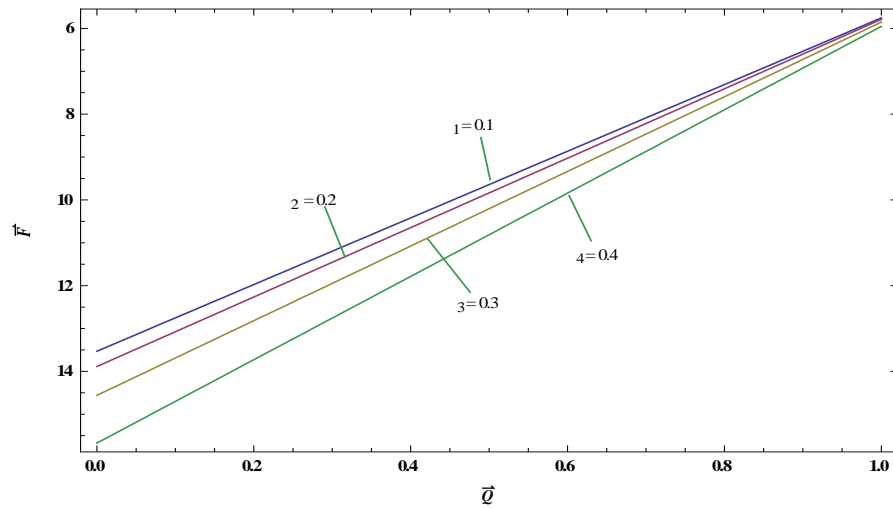


**Figure 3(d).** Effect of  $\bar{Q}$  and  $\bar{F}$  ( $N_b = 0.3, N_t = 0.8, G_r = 0.2, B_r = 0.3, \alpha = 30^\circ, \epsilon = 0.4, F = 0.1, k = 0.04, \lambda = 0.01, a_0 = 0.01$ )

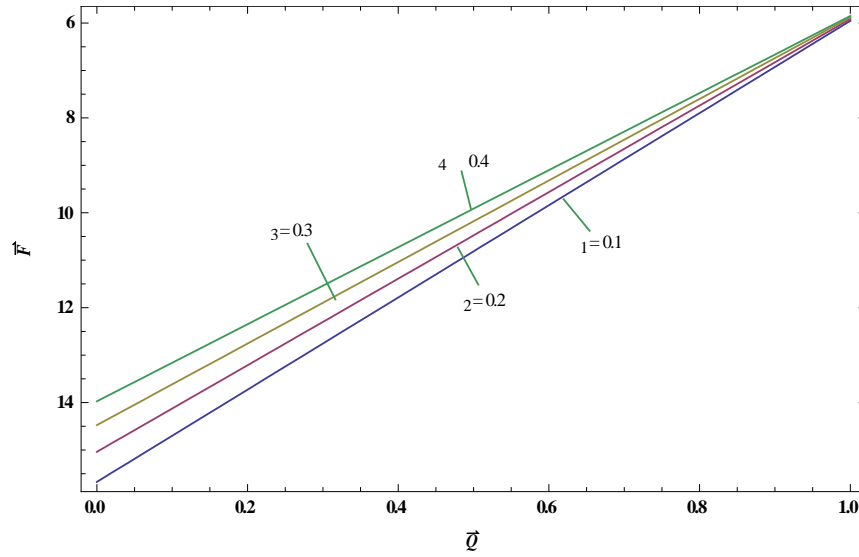


**Figure 3(e).** Effect of  $\bar{Q}$  and  $\bar{F}$  ( $N_b = 0.3, N_t = 0.8, G_r = 0.2, B_r = 0.3, \alpha = 30^\circ, \epsilon = 0.4, F = 0.1, k = 0.04, a_0 = 0.01, \phi = 0.4$ )

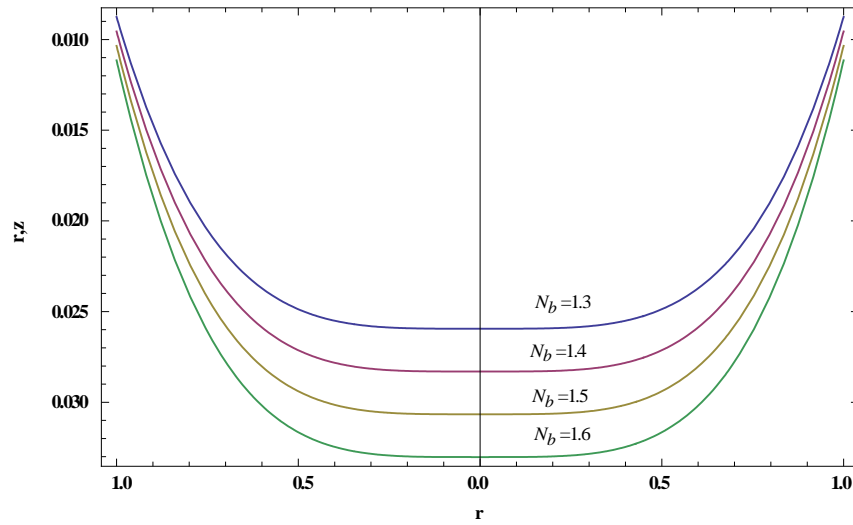


**Figure 4(a).** Effect of  $r$  and  $\theta(r, z)$  ( $k = 0.04, \lambda = 0.05, a_0 = 0.03, \phi = 0.1, N_t = 0.2, z = 0.2$ )

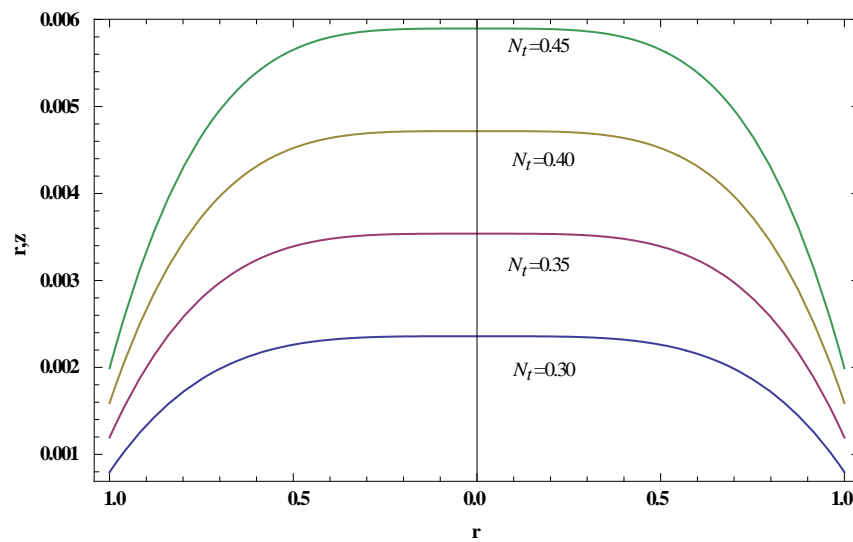


**Figure 4(b).** Effect of  $r$  and  $\theta(r, z)$  ( $k = 0.04, \lambda = 0.05, a_0 = 0.03, \phi = 0.1, N_b = 0.2, z = 0.2$ )



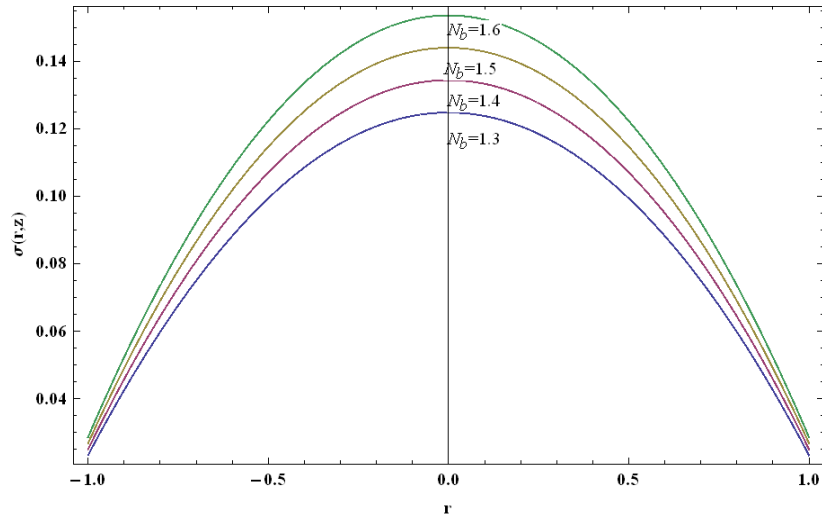


**Figure 5(a).** Effect of  $r$  and  $\sigma(r, z)$  ( $k = 0.04, \lambda = 0.05, a_0 = 0.03, \phi = 0.1, N_t = 0.2, z = 0.2$ )

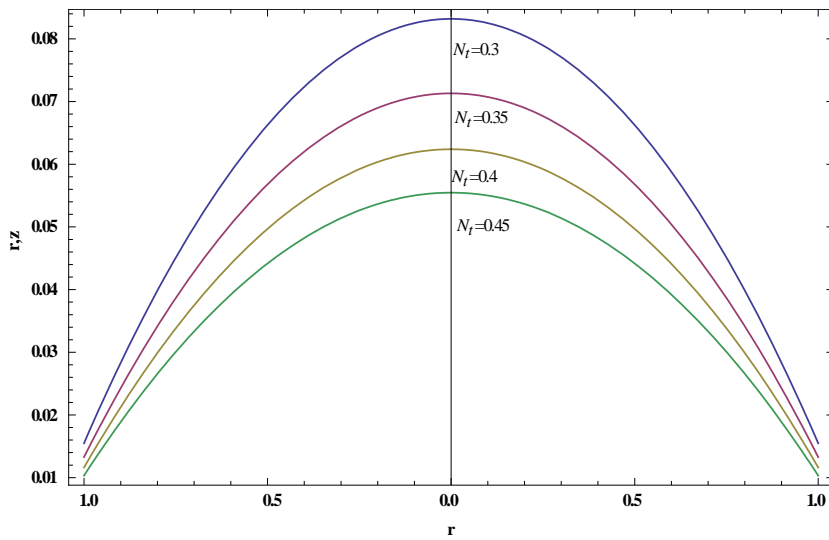


**Figure 5(b).** Effect of  $r$  and  $\sigma(r, z)$  ( $k = 0.04, \lambda = 0.05, a_0 = 0.03, \phi = 0.1, N_b = 1.3, z = 0.2$ )

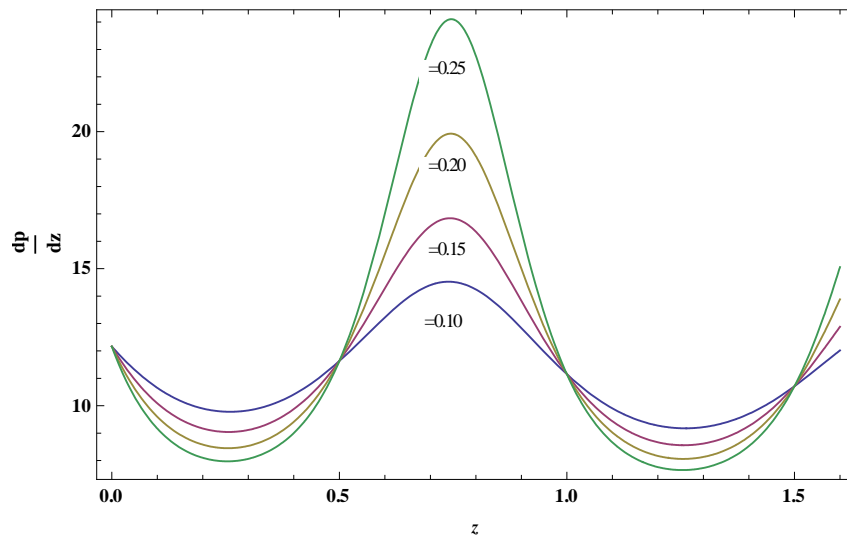


**Figure 6(a).** Pressure gradient versus Sinusoidal wave ( $k = 0.04, \lambda = 0.01, a_0 = 0.01, G_r = 0.2, B_r = 0.3, N_b = 0.3, N_t = 0.8, Q = 0.2$ )

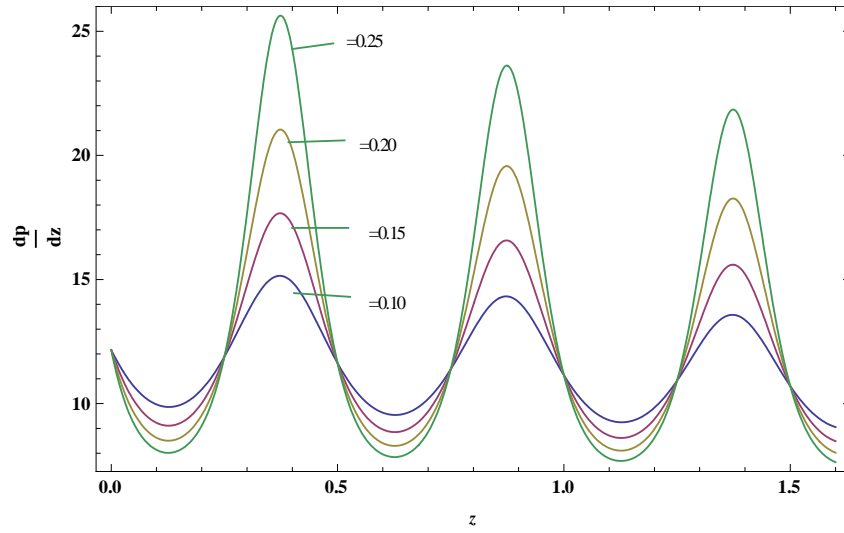


**Figure 6(b).** Pressure gradient versus multi Sinusoidal wave ( $k = 0.04, \lambda = 0.01, a_0 = 0.01, G_r = 0.2, B_r = 0.3, N_b = 0.3, N_t = 0.8, Q = 0.2$ )

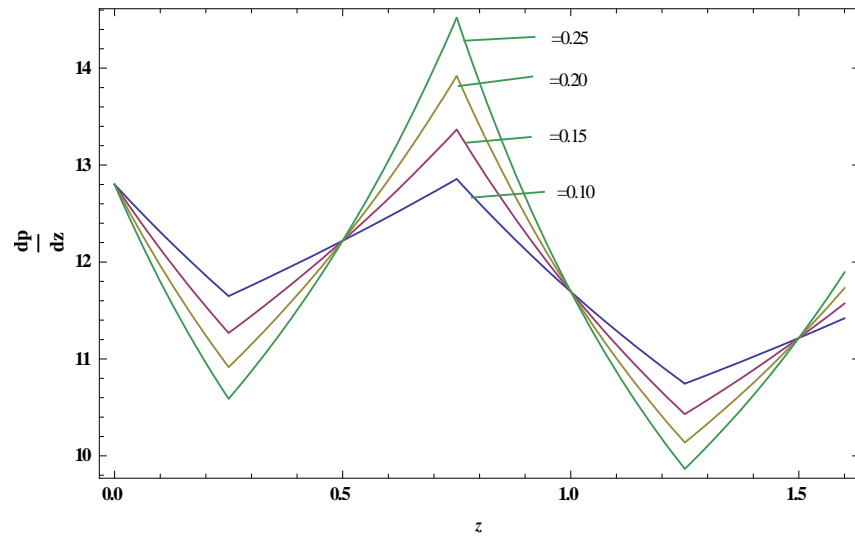


**Figure 6(c).** Pressure gradient versus Triangular wave ( $k = 0.04, \lambda = 0.01, a_0 = 0.01, G_r = 0.2, B_r = 0.3, N_b = 0.3, N_t = 0.8, Q = 0.2$ )

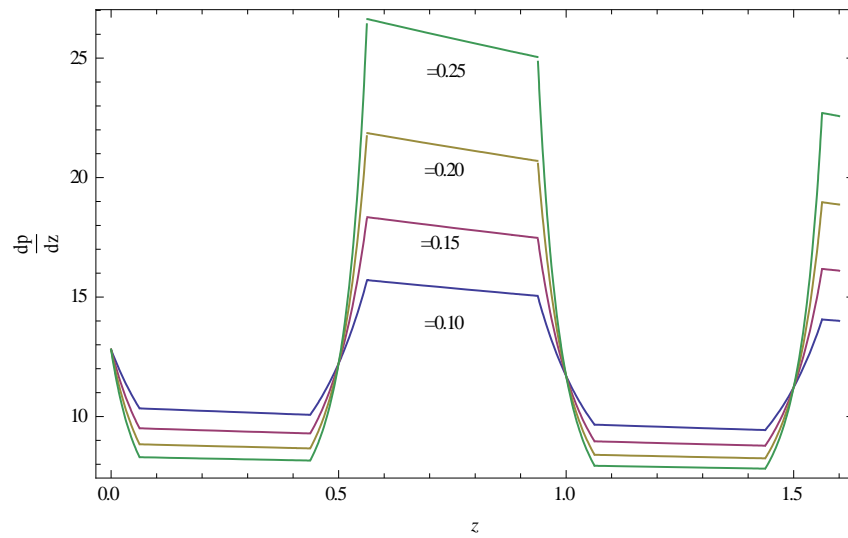


**Figure 6(d).** Pressure gradient versus Trapezoidal wave ( $k = 0.04, \lambda = 0.01, a_0 = 0.01, G_r = 0.2, B_r = 0.3, N_b = 0.3, N_t = 0.8, Q = 0.2$ )

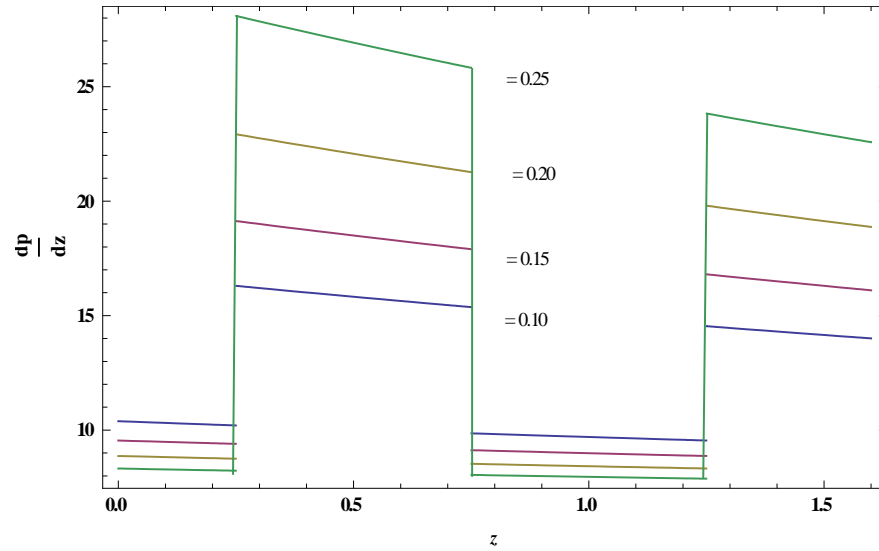


**Figure 6(e).** Pressure gradient versus Square wave ( $k = 0.04, \lambda = 0.01, a_0 = 0.01, G_r = 0.2, B_r = 0.3, N_b = 0.3, N_t = 0.8, Q = 0.2$ )

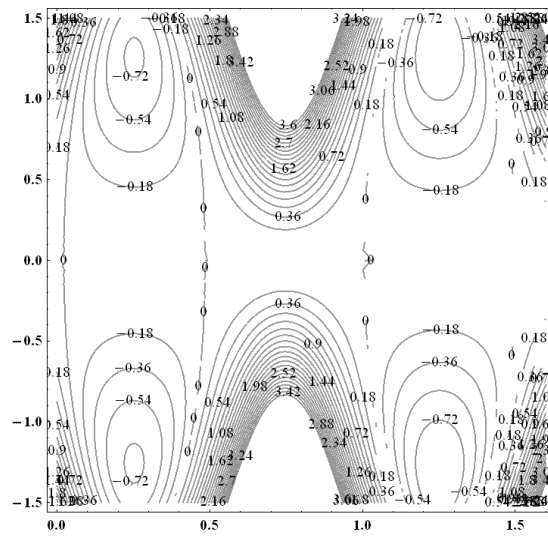


**Figure 7(a).** Stream lines for Sinusoidal wave ( $\lambda = 0.01, a_0 = 0.01, k = 0.04, \phi = 0.4, \alpha = 30^\circ, B_r = 0.3, G_r = 0.2, N_b = 0.3, N_t = 0.8, F = 0.1, \epsilon = 0.2, Q = 0.2$ )

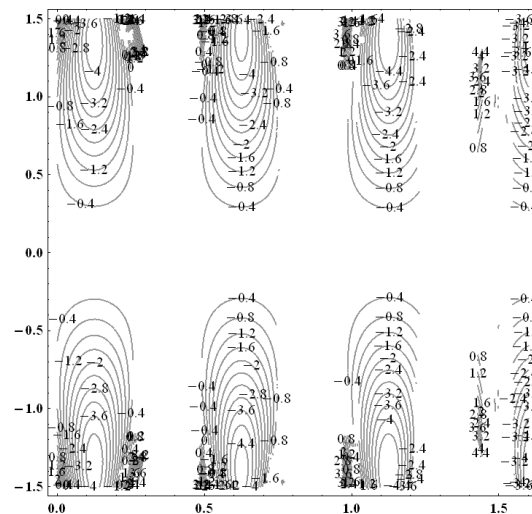


**Figure 7(b).** Stream lines for Multi Sinusoidal wave ( $\lambda = 0.01, a_0 = 0.01, k = 0.04, \phi = 0.4, \alpha = 30^\circ, B_r = 0.3, G_r = 0.2, N_b = 0.3, N_t = 0.8, F = 0.1, \epsilon = 0.2, Q = 0.2, m = 2$ )

## 6. Conclusions

This study examines the peristaltic transport of a nanofluid passing through an inclined tube under the long wave length and low Reynolds number assumptions. Temperature profile and nanoparticle phenomena have been calculated using Homotopy Perturbation technique while analytical solutions have been calculated for velocity profile, pressure drop, time averaged flux and frictional force. Pressure gradient versus wave amplitude for various waves have been represented.

The main points of the analysis are as follows:

- The pressure drop increases with the Brownian motion number ( $N_b$ ), whereas decreases with the thermophoresis parameter ( $N_t$ ) and inclination ( $\alpha$ ). Pressure drop decreases with wave amplitude ( $\phi$ ) and increases with wave length ( $\lambda$ ) but converges to a certain point after  $\bar{Q}$  exceeds one.
- The frictional force increases with the Brownian motion number ( $N_b$ ), whereas decreases with the thermophoresis parameter ( $N_t$ ) and inclination ( $\alpha$ ). Frictional force decreases with wave amplitude ( $\phi$ ) and increases with wave length ( $\lambda$ ) but converges to a particular value after  $\bar{Q}$  is one.
- The frictional force has a similar behaviour compared to the pressure drop.
- The temperature profile decreases with the Brownian motion number ( $N_b$ ) and increases with the thermophoresis parameter ( $N_t$ ).
- The nanoparticle phenomena increases with the Brownian motion number ( $N_b$ ) and decreases with the thermophoresis parameter ( $N_t$ ).
- The temperature profile has an opposite behaviour compared to nanoparticle phenomena.
- For sinusoidal, triangular and trapezoidal waves, maximum pressure gradient occurred for  $z \in [0.5, 1]$  with increase in wave amplitude. For square wave, it is for  $z \in [0.25, 0.75]$  and multi sinusoidal wave it is for  $z \in [0.25, 0.5]$ .
- The size of the trapped bolus in multi sinusoidal wave is small as compared to the sinusoidal wave.

## ACKNOWLEDGEMENTS

The authors wish to thank the referees for their valuable and constructive comments which lead to significant improvement of the paper.

## REFERENCES

- [1] Buongiorno J, Convective transport in nanofluids, ASME J Heat Transf. 128 (2006) 240-250.
- [2] Choi SUS, Enhancing thermal conductivity of fluids with nanoparticles, In: Siginer DA, Wang HP (eds) Developments and applications of Non-Newtonian flows, ASME, New York, 66 (1995) 99-105.
- [3] Das SK, Putra N, Roetzel W, Pool boiling of nano-fluids on horizontal narrow tubes, Int. J. Multiph. Flow 29 (2003) 1237-1247.
- [4] Devi RG, Devanathan R, Peristaltic motion of a micro polar fluid, Proc. Indian Acad. Sci. 81A (1975) 149-163.
- [5] Fung YC, Yih CS, Peristaltic transport, J. Appl. Mech. Trans. ASME 5 (1968) 669-675.
- [6] He JH, Application of homotopy perturbation method to nonlinear wave equations, Chaos Solitons Fractals 26 (2005) 695-700.
- [7] He JH, Approximate analytical solution for seepage flow with fractional derivatives in porous media, Comput. Methods Appl. Mech. Eng. 167 (1998) 57-68.
- [8] He JH, Homotopy perturbation technique, Comput. Methods Appl. Mech. Eng. 178 (1999) 257-262.
- [9] Khan WA, Pop I, Boundary-layer flow of a nanofluid past a stretching sheet, Int. J. Heat Mass Transfer 53 (2010) 2477-2483.
- [10] Kuznetsov AV, Nield DA, Natural Convective boundary layer flow of a nanofluid past a vertical plate, Int. J. Thermo Sci. 49 (2010) 243-247.
- [11] Latham TW, Fluid motion in a peristaltic pump, MS. Thesis, Massachusetts Institute of Technology, Cambridge (1996).
- [12] Maruthi Prasad K, Radhakrishnamacharya G, Flow of Herschel – Bulkley Fluid in an inclined tube of Non-Uniform Cross-Section with Multiple Stenoses, Arch. Mech. 60(2) (2008) 159-170.
- [13] Maruthi Prasad K, Radhakrishnamacharya G, J V Ramana Murthy, Peristaltic pumping of a micropolar fluid in an inclined tube, Int. journal of Appl. Math and Mech. 6(11) (2010) 26-40.
- [14] Maruthi Prasad K, Ramana Murthy JV, VK Narla, Unsteady Peristaltic Transport in Curved Channels, Physics of Fluids, 25 (2013) 091903, DOI:10.1063/1.4821355.
- [15] Mekheimer Kh S, Peristaltic Flow of Blood under Effect of a Magnetic Field in a Non-Uniform Channels, Appl. Math. Comput. 153 (2004) 763-767.
- [16] Misra M, Rao AR, Peristaltic Transport of a Newtonian Fluid in an Asymmetric Channel, ZAMM 54 (2003) 532-550.
- [17] Muthu P, Ratish Kumar BV, Chandra P, On the influence of wall properties in the peristaltic motion of micro polar fluid, ANZIAM J. 45 (2003) 245-260.
- [18] Noreen Sher Akbar, Nadeem S, T Hayat, Awatif a. Hendi, Peristaltic flow of a nanofluid in a non-uniform tube, Heat and Mass Transfer 48 (2011) 451-459.
- [19] Radhakrishnamacharya G, Srinivasulu Ch, Influence of Wall Properties on Peristaltic Transport with heat transfer, Comptes Rendus Mechanique 335 (2007) 460-480.
- [20] Shapiro AH, Jaffrin MY, Weinberg SL, Peristaltic pumping with long wavelengths at low Reynolds numbers, J. Fluid Mech. 37 (1969) 799-825.
- [21] Srivastava LM, Srivastava VP, Peristaltic Transport of Blood: Casson Model II, J. Biomech. Eng. 104 (1982) 182-189.